

# PV MODULE RELIABILITY SCORECARD - ROUND 1

**Lawrence Pratt<sup>1</sup>, Manjunath Basappa Ayanna<sup>2</sup>, Siyasanga Innocent May<sup>2</sup>,  
Wisani Mkasi<sup>2</sup>, Loyiso Maweza<sup>2</sup>, Kittessa Roro<sup>2</sup>**

<sup>1</sup> Council for Scientific and Industrial Research (CSIR), Pretoria, South Africa,  
Phone: +27 060 688 5929, E-Mail: [lp Pratt@csir.co.za](mailto:lp Pratt@csir.co.za)

<sup>2</sup> CSIR; E-mail: [MBasappaAyanna@csir.co.za](mailto:MBasappaAyanna@csir.co.za), [SMay@csir.co.za](mailto:SMay@csir.co.za), [HMkasi@csir.co.za](mailto:HMkasi@csir.co.za),  
[LMaweza@csir.co.za](mailto:LMaweza@csir.co.za), [kroro@csir.co.za](mailto:kroro@csir.co.za)

**Abstract:** Solar PV system component reliability is key to long-term success for the PV industry, given the 25-year lifespan of PV generators. PV modules are one key component needed to deliver on the lifetime production of PV systems, as they are the engines that convert the fuel from the sun into the electrons for use here on Earth. This research presents the results from the first round of reliability testing for commercially available PV modules based on accelerated stress tests conducted at the CSIR Energy Centre. Four module types with a specific bill of materials (BOM) were subjected to a series of accelerated stress tests as defined by the C450 international standard. Pre- and post-stress characterizations were conducted to quantify the changes in safety and performance due to the accelerated stress. PV module power decreased by less than 3% for all modules subjected to mechanical loads, humidity-freeze, thermal cycling, and PID. However, the degradation rates among the four BOMs differed significantly ( $p < 0.001$ ) following the thermal cycling sequence. PV module power decreased by as much as 9% following the damp heat stress prior to the final stabilization. The work was conducted to demonstrate the value of accelerated stress testing now available in South African to support the PV industry. The round one results highlight potential differences in the long-term performance of PV module BOMs in the field, supporting the value of accelerated stress testing to de-risk investments in PV generators.

*Keywords: PV module, quality, reliability, accelerated stress test, electrical performance, safety, IEC.*

## 1. Introduction

The CSIR Energy Centre Solar Photovoltaic Quality and

Reliability Test Laboratory (PQRL) conducted a reliability pilot program on four distinct PV module bill of materials (BOMs) beginning in 2019. This paper describes the test flow, test procedures, and the test results anonymously to protect the brand identities, both foreign and domestic. Each sequence in the reliability program is designed to accelerate specific field failures known to occur on crystalline silicon modules over years in the field, so that long-term reliability may be simulated, and PV models may be ranked according to the loss in power resulting from the stress tests.

The reliability pilot program was funded by the CSIR Energy Centre with module donations coming from the participants in exchange for test results. Thirteen (13) modules were selected at random and assigned to various test sequences. Performance and safety tests were conducted prior to the stress tests to establish a baseline and again at multiple stages throughout the test sequence to quantify changes in electrical performance and safety caused by each accelerated stress. The final ranking of PV models is based on the power loss between the initial and final characterization.

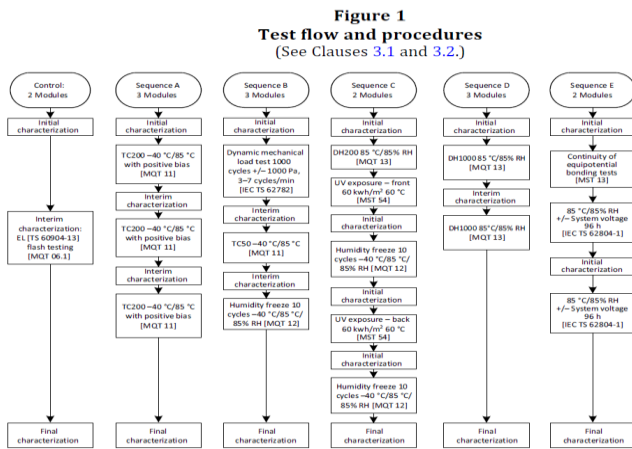
The reliability test program provides quantitative data that can be used to rank the PV modules included in the test protocol. The PVEL PV Scorecard [1] provides an example of how the global PV industry interest in ranking and rating of PV modules based on results from accelerated stress testing. The reliability program can identify PV modules that exhibit unusual electrical performance or safety test degradation after accelerated stress tests in weeks instead of years. The test results should correlate with the long-term reliability of PV modules by accelerating typical field failures that might otherwise take years to develop and help to identify modules that are particularly susceptible to degradation in the field. PV module manufacturers use these

results to identify areas for improvement in product reliability and market independently verified reliable products. PV plant developers and owners use these results at the procurement stage to reduce the risk of under-performance over the lifetime of the PV plant.

## 2. Method

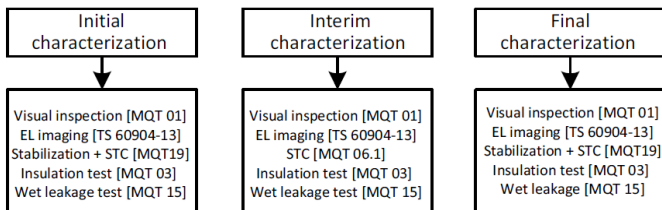
### 2.1. Test Procedures

Figure 1 shows the PV module reliability test sequence as defined by the CSA/ANSI C450-18 standard [2]. This test sequence is the first publicly available standard for long-term reliability testing for solar PV modules. The C450 standard development committee represented a broad range of participants from the PV industry. The C450 standard is a collection of tests defined in the IEC 61215-2 for PV module type qualification [3], IEC 61730-2 for PV module safety [4], TS 60904-13 for electroluminescence imaging [5], and IEC TS 62804-1 for potential induced degradation (PID) [6].



**Figure 1. The C450 test sequence for PV module reliability testing**

Figure 2 below shows the characterization steps included in the C450 sequence, with reference to the relevant standard and sections.



**Figure 2. Characterization steps conducted before and after stress tests**

### 2.2. Test Descriptions

This section provides a brief description of each test conducted as part of the C450 test sequence. The stress tests are designed to provoke specific failures observed in fielded modules over time. The stress tests include thermal cycling (TC), humidity-freeze (HF), damp heat (DH), dynamic mechanical load (DML), and potential induced degradation (PID). The characterization steps are designed to quantify the results of the stress. The characterization steps include visual inspection, electroluminescence imaging (EL), electrical performance at standard test conditions (STC), dry insulation resistance safety test, and the wet leakage current safety test. This section briefly describes the characterization steps first, followed by the stress tests.

#### 2.2.1. Visual Inspection, IEC 61215:2016 MQT 01

The visual inspection of each module serves to document any visual changes due to the stress tests, such as cracks, bubbles in the backsheet, scratches or delamination, etc. which may impact the module performance.

#### 2.2.2. Electroluminescence imaging IEC 60904-13

The electroluminescence (EL) image of the PV module serves to document changes in the module that are not visible to the naked eye, especially cracks and inactive cells. The EL image of a PV module is similar in purpose to an x-ray for a human skeleton. The module is connected to DC power supply in a forward bias condition and current equal to the rated short circuit current ( $I_{sc}$ ) is applied. The image is taken in the dark with a specially filtered camera to capture emissions in the 1100 nm wavelength range.

#### 2.2.3. Performance at STC, IEC 61215:2016 MQT 6.1

The electrical performance of the PV module at standard test conditions (STC) serves to document changes in the power output due to the stress test. The current-voltage (IV) curve of the PV module is recorded using a Class A+A+A+ indoor sun simulator at a cell temperature of  $25 \pm 2$  °C, irradiance of  $1000 \pm 2$  W/m<sup>2</sup> and air mass of 1.5. Several summary statistics are extracted from each IV curve, including, to quantify changes in the electrical performance.

#### 2.2.4. Insulation Resistance, IEC 61215:2016 MQT 03

The electrical insulation test serves to document changes in the electrical safety of each module under high voltage bias and dry conditions due to the stress test. To conduct the test, a module is connected to a DC power supply and biased at the maximum system voltage (1000 V or 1500 V) plus twice the maximum system voltage for one (1) minute. Then the voltage bias is reduced to the maximum system voltage, held for two (2)

minutes, and the insulation resistance is recorded.

#### 2.2.5. Wet Leakage current test MQT 15 IEC 61215:2016

The wet leakage test serves to document changes in the electrical safety of each module under high voltage bias and wet conditions due to the stress test. The module is immersed in water with resistivity less than 3500  $\Omega$  and temperature of 22 ( $\pm 2$ ) °C. The maximum system voltage is applied for two (2) minutes and the insulation resistance is recorded. The insulation resistance must exceed a certain minimum threshold to ensure no dangerous levels of current can flow between the internal electrical circuit and accessible parts.

#### 2.2.6. Thermal cycling, IEC 61215:2016 MQT 11

Thermal cycling (TC) tests the ability of the PV module to withstand the thermal stresses associated with changes in temperatures over the course of the day and the seasons. The module is loaded in an environmental chamber and subjected to 200 temperature cycles ranging from -40 °C to +85 °C. An electrical bias equivalent to the module current at maximum power is applied to the module during the ramp up from -40 °C to +80 °C to simulate the electrical flow inside the circuit that occurs naturally in the sunlight. The stress is designed to provoke broken interconnects, broken cells, electrical bond failures, junction box adhesion failures, and open circuit-potential leading to arcing.

#### 2.2.7. Humidity Freeze, IEC 61215, MQT 12

Humidity-freeze (HF) tests the ability of the PV module to withstand damp heat stress in combination with freezing conditions. The module is loaded in the environmental chamber and subjected to 85 °C and 85% relative humidity (RH) for 20 hours followed by a four (4) hour freeze cycle at -40 °C for 30 minutes. The sequence is repeated for ten (10) cycles. The stress is designed to provoke delamination of the encapsulant, junction box adhesion failures, and inadequate edge deletion.

#### 2.2.8. Damp Heat Testing, IEC 61215:2016 MQT 13

Damp heat (DH) tests the ability of the PV module to withstand damp heat stress associated with hot, humid environments. The PV module is loaded into an environmental chamber and exposed to 85% relative humidity (RH) and 85°C for 1000 hours. The stress is designed to provoke corrosion, delamination, encapsulant loss of adhesion & elasticity, and junction box adhesion failures.

#### 2.2.9. Dynamic Mechanical Load Testing IEC TS 62782

The dynamic mechanical load (DMLT) tests the ability of the PV module to resist micro-cracks. The module is fastened to a test

jig designed to simulate typical mounting configurations in the field. A 1000 Pa load is applied to the module downward and upward at a rate of 3-7 cycles per minute for 1000 cycles. This is used to provoke micro cracks in the solar cells that may worsen under subsequent thermal cycling and humidity freeze (HF).

#### 2.2.10. Potential Induced Degradation, IEC TS 62804-1 MST 13

The potential induced degradation (PID) tests the ability of the PV module to resist leakage current under damp conditions in the presence of high electrical bias. This phenomenon occurs early in the mornings when condensation has collected on the PV module glass and the inverter has not yet initialized. To simulate this condition, the module is loaded into an environmental chamber and subjected to 85% RH and 85°C for 96 hours with an electrical bias of 1000 or 1500 V between the circuit and the frame, depending on the maximum rated system voltage specified by the manufacturer. The PID stress is designed to provoke the leakage path between the internal circuit and the frame, which can lead to significant loss of power in the PV plant.

### 3. PV modules

The PV modules were solicited from various suppliers willing to provide samples free of charge in exchange for test results. A total of four (4) PV module BOMs were tested simultaneously in the lab, and well-known PV module brands were included in the pilot program from both foreign and domestic brands. Table 1 shows some characteristics of the PV modules included in the test, along with an anonymous label used throughout the article for reference.

**Table 1. Module characteristics of four (4) PV module models included in the pilot program**

ID	Pmp (W)	Cell type	# of cells	Bifacial
19034	375	mono-PERC	72	Yes
19040	320	multi	72	No
19047	385	multi-PERC	72	No
19058	300	mono	72	No

The detailed BOM used in the construction of each PV module tested was not made available from all participants. Two of the models were constructed with passivated emitter rear-contact (PERC) cells according to the company contact, although the

CSIR was not able to independently verify. The rest of the characteristics were easily verified by inspection. The BOM details are necessary to consider when attempting to make inference on the larger population of PV modules from which these samples were selected, as not all PV modules with identical model numbers are constructed with the same BOM. PV manufacturers often substitute suppliers and optimize process parameters over the production lifetime of a PV model, and long-term performance in field may vary because of changes in the BOM.

Furthermore, the PV modules tested in this pilot program were not based on a random sample of the population. Given the lack of transparency regarding the BOM and the lack of randomness in the sample selection, the results of this pilot program tests are strictly limited in terms of broad inference on the larger population of modules. Rather the results should be viewed as indicative of the types of failures that can occur during accelerated stress testing. Results based on accelerated stress tests are informatize when conducted on batches of modules selected at random from production runs that are planned for specific projects with a specific BOM. Under these conditions, inference can be made about the performance of the entire production run subjected to the same sequence of tests.

## 4. Test Results and discussion

### 4.1. Visual Inspection

All modules were visually inspected at the start of the test sequence and following each stress test. Nothing remarkable was noted at initial visual inspection or final visual inspection.

### 4.2. EL Images

EL images for all modules were captured during initial characterization and following each stress test. In general, the EL images remained unchanged over the test sequence with a few cracked cells noted on some modules. BOM 19058, however, exhibited an unusual number of cracked cells during the TC600 sequence. Figure 3 shows the initial and post TC600 EL images for 19058-03, one of the three modules subjected to this sequence. Nineteen (19) cracked cells were noted following TC600 where none existed at the initial inspection. **Error! Reference source not found.** also shows the cumulative number of cracked cells across all three modules after TC600 by position. The cells in the upper left corner and bottom right corner tended to crack more the cells in other positions.

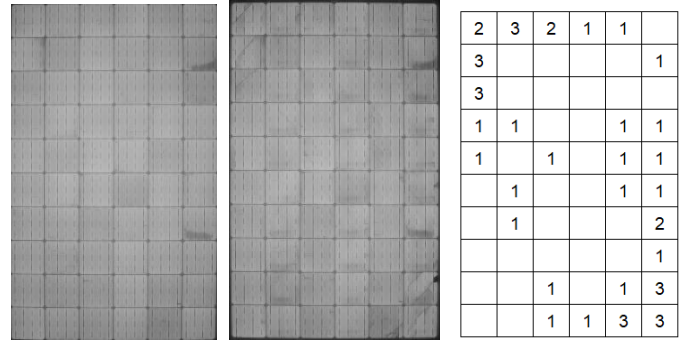


**Figure 3. EL images of 19058-03 at initial, post TC200, post TC400, and post TC600**

### 4.3. Electrical Performance

Figure 4 shows the change in maximum power (Pmp) relative to the initial power measurement for each module following each stress test. The results are grouped by test sequence starting with the damp heat (DH) on the left and ending with the thermal cycling (TC) on the right. The grey horizontal lines represent +/- 1%, and the thick black line represents the 5% pass/fail criteria for PV module qualification tests. The colors represent the four BOMs and there are two or three measurements per BOM per stage.

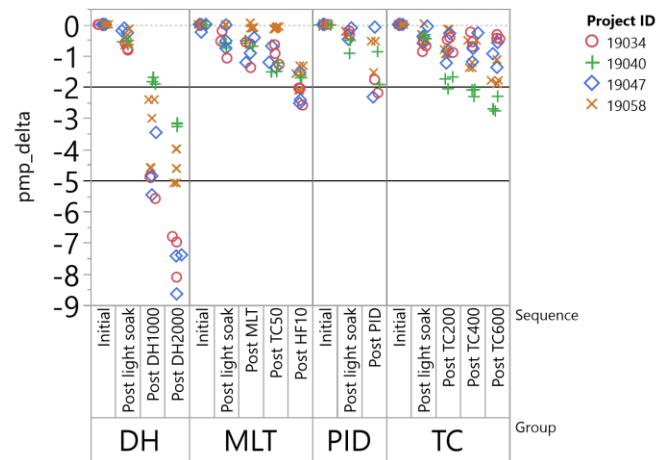


**Figure 4. Change in maximum power (Pmp) relative to initial Pmp for BOM 19034 (red), 19040 (green), 19047 (blue), and 19058 (orange).**

#### 4.3.1. Initial IV and post stabilization:

Initial IV measurements at STC were conducted on the modules as received and after stabilization process in natural sunlight to establish baseline IV characteristics. The initial measurement serves as a baseline reference to quantify the degradation in each module after each stress test. The measured degradation in Pmp decreased by as little as 0.2% for BOM 19058 and as much as 0.6% for BOM 19034 due to the outdoor light stabilization, on

average.

#### 4.3.2. Sequence A, Thermal Cycling test (TC):

Three modules from each BOM were subjected to thermal stress at intervals of two hundred cycles each: TC200, TC400 and TC600. The measured maximum power (Pmp) decreased by less than 3% relative to initial for all four BOMs after TC600. However, the power loss was significantly different among the four BOMs after TC600 ( $p < 0.001$ ). BOM 19034 measured the least degradation (0.4%, on average) and BOM 19040 measured the most degradation (2.6%, on average). The difference in maximum power loss among the BOMs correlates strongly to difference in Vmp losses.

The thermal cycling stress accelerates the impacts from temperature changes in the field resulting from day/night cycles and fluctuations in irradiance due to passing clouds. The TC600 exposed the PV modules to 600 extreme temperature cycles, and 600 day/night cycles occur over 1.6 years in the field. Assuming a 1:1 relationship between the 600 cycles in the chamber and 600 day/night cycles in the field, then module power for BOM 19034 would degrade by 0.25% per year while module power for BOM 19040 would degrade by 1.6 % per year in the field. While the relationship between power loss under accelerated stress versus power loss in the field is by no means a certainty, this does provide some indication that one might could be more durable than another over the useful lifetime of the PV module.

#### 4.3.3. Sequence B, DMLT/TC50/HF10:

Three modules from each BOM were subjected to a sequential stress sequence in this order: Dynamic Mechanical Load Testing (DMLT), Thermal Cycling (TC), and Humidity Freeze (HF). The Pmp decreased by 0.5% on average relative to initial Pmp after DMLT stress test. Most of this decrease had already occurred following the outdoor light soaking. The Pmp decreased by less than 0.5% on average following the TC50 stress test. Finally, the measured Pmp decreased by approximately 1 % on average follow the HF10. The decrease in Pmp was not significantly different for any of the four BOMs at the 5% significance level ( $p = 0.08$ ).

#### 4.3.4. Sequence D, Damp Heat:

Three modules from each BOM were subjected to high temperature and high humidity stress tests over two intervals of 1000 hours each. After DH2000, the decrease in Pmp was significantly less for BOMs 19040 and 19058 constructed with standard cells compared to the decrease in Pmp for BOMs 19034

and 19047 ( $p < 0.0001$ ) which were constructed from PERC cells. To address concerns over potential impacts from the test procedure itself, the latest draft of IEC 61215 includes a stress specific stabilization procedure to reverse boron-oxygen defects that may become artificially active due to the damp heat stress conditions. The modules from all four BOMs were stabilized at 80 C for 48 hours with electrical bias, according to the draft standard. The subsequent IV tests showed an increase in Pmp for both PERC cell BOMs and one of the two standard cell BOMs. The Pmp for BOM 19040 decreased by 5% compared to the previous measurement, which was unexpected. Further analysis and research are required to understand the implications of the damp heat sequence.

#### 4.3.5. Sequence E, Potential Induced Degradation (PID):

Two modules from each BOM were subjected to high temperature and high humidity stress for 96 hours each while under electrical bias between the cells and the frame. Due to shut down related to the national lockdown, only one of the two intervals was completed. The measured Pmp decreased by less than 2.5% relative to initial for all modules and no significant difference was observed among the BOMs.

#### 4.3.6. Control Modules:

Two control modules from each BOM were kept in the sun simulator work area throughout the test sequence. The control modules were measured to validate the stability of the measurement system every time before any stress test modules were measured to confirm that significant shifts in IV characteristics of tested modules were due to the stress and not due to a drift in the measurement system. The control modules were stable and measured within the +/- 0.5% control limits during the test sequence for three out of four BOMs, indicating the measurement system was stable. The maximum power for BOM 19047 control modules decreased by 1.1% over the course of the test sequence, suggesting some electrical instability in the BOM.

### 4.4. Insulation Resistance

All the modules were subjected to the dry insulation resistance test following each stress test, and none failed for safety at any stage. All insulation resistance measurements were above the pass/fail threshold of 20-25 MΩ at maximum system voltage. The results indicate that the insulation resistance between live parts and accessible parts is sufficiently high to meet the

requirements for PV module qualification according to IEC standards, even after all the additional stress tests.

#### 4.5. Wet Leakage Current Test

All the modules were subjected to the wet leakage current safety test at every stage, and none failed for safety at any stage. All insulation resistance measurements exceeded the pass/fail threshold of 20-25 M $\Omega$ , depending on the area of the PV module. These results indicate that the wet leakage current resistance between live parts and accessible parts is sufficiently high to meet the requirements for PV module qualification according to IEC standards, even after all the additional stress tests.

### 5. PV Scorecard

Table 2 shows a simple PV scorecard that summarizes the relative performance for each BOM based on the decrease in Pmp after the final characterization relative to the initial Pmp, sorted by project ID. A one (1) corresponds to the lowest Pmp loss among the four (4) BOMs for a given sequence and a four (4) corresponds to the highest Pmp loss for that sequence. The totals show the sum of the ranks from each sequence A, B, D, and E using both the Pmp loss for sequence D measured after the DH2000 and measured after the BO stabilization treatment. The ranks remain relatively stable for three out of four BOMs with both approaches, but BOM 19040 moves from second best to worst performer when the BO stabilization is included. This was the only BOM to show power loss after the BO stabilization process. The value and the relevance of the BO stabilization is debated among experts but the impact on the rankings in the scorecard is significant. BOM 19058 is ranked best using both metrics.

**Table 2. PV scorecard showing the ranks of each BOM for each sequence based on the power loss between initial and final characterization with lower scores corresponding to lower power loss**

Project	A	B	D DH2000	D BO LID	E	Total after DH2000	Total after BO
19034	1	4	3	2	4	12	11
19040	4	1	1	4	3	9	12
19047	2	3	4	3	2	11	10
19058	3	2	2	1	1	8	7

The PV scorecard is an oversimplification of the electrical performance results, but perhaps a useful tool as the number of BOMs in the database grows. The PVEL PV Scorecard does rank PV models for each test sequence but does not attempt to rank across all sequences combined to provide one score.

The PV scorecard may also be extended to include other results in addition to the electrical performance. For example, BOM 19058 proved to be most durable in terms of electrical performance yet exhibited unusual crack patterns during the TC600 sequence. The number of cracked cells could be included in scorecard, despite the low impact on the electrical performance. In that case, the extent of the cracks, the orientation of the cracks, and the resultant inactive regions should also be considered, as these factors can impact the degree of power loss [7]. The PVEL PV Scorecard does not explicitly rank according to the cracked cells, but EL images do feature in the summary report to show the changes that occur because of humidity-freeze, PID, and other stresses. The safety tests could also be incorporated. In this pilot, all the modules passed the electrical safety tests, so there was no distinction among the BOMs. However, should an electrical safety test failure occur, how does that result get incorporated into the ranking? In the end, the PVEL PV Scorecard approach may strike the correct balance by ranking all the models by stress sequence and avoiding a single, combined score.

### 6. Conclusion

The first extended reliability test program at the CSIR PV module quality and reliability was completed in 2019-2020. The results demonstrate the capability to deliver accelerated stress test results to evaluate the relative performance of PV module brands, both foreign and domestic. The power output from the four (4) BOMs tested degraded by less than 3% following a defined test protocol that included thermal stress, humidity-freeze stress, dynamic mechanical stress, and potential induced degradation. The power loss from the damp heat stress was ambiguous, as three out of four BOMs recovered most of the power loss from damp heat when followed by a stabilization process. The power loss for modules from the fourth BOM increased following the stabilization process. The relative ranking in the PV scorecard was impacted by the results from the stabilization procedure.

The reliability pilot program demonstrated a new capability for the CSIR to support the local PV industry. Accelerated stress testing for PV modules is now available locally for decision support regarding PV module procurement, batch testing for independent verification of PV module reliability, and troubleshooting field failures.

## Acknowledgements

The authors wish to thank the CSIR executive committee and the Technology Localization and Implementation Unit (TLIU) of the Department of Science and Technology (DST) for the generous support and funding necessary to design, build, and operate the PV module quality and reliability test lab in Pretoria. The lab provides a unique testing service in all of southern Africa to support the local PV industry now and in the future as the share of electricity generation from solar PV continues to expand.

## References

- [1] PVEL, 2020, PV-Module-Reliability-Scorecard.pdf, <https://www.pvel.com/wp-content/uploads/2020-PVEL-PV-Module-Reliability-Scorecard.pdf> (accessed May 28, 2020).
- [2] CSA/ANSI, "Photovoltaic (PV) module testing protocol for quality assurance programs." CSA/ANSI, 2018.
- [3] IEC, "IEC 61215-2 Terrestrial photovoltaic (PV) modules – Design qualification and type approval – Part 2: Test procedures." 2016.
- [4] IEC, "IEC 61730-2 Photovoltaic (PV) module safety qualification – Part 2: Requirements for testing." 2016.
- [5] IEC, "IEC TS 60904-13 Photovoltaic devices – Part 13: Electroluminescence of photovoltaic modules." 2018.
- [6] IEC, "IEC 62804-1 Photovoltaic (PV) modules – Test methods for the detection of potential-induced degradation – Part 1: Crystalline silicon." 2015.
- [7] M. Bdour, Z. Dalala, M. Al-Addous, A. Radaideh, and A. Al-Sadi, A Comprehensive Evaluation on Types of Microcracks and Possible Effects on Power Degradation in Photovoltaic Solar Panels, *Sustainability*, vol. 12, no. 16, p. 6416, Aug. 2020, doi: 10.3390/su12166416.